

Stiffness and thermal expansion of ZrB_2 : an *ab initio* study

This article has been downloaded from IOPscience. Please scroll down to see the full text article.

2005 J. Phys.: Condens. Matter 17 2233

(<http://iopscience.iop.org/0953-8984/17/13/019>)

View [the table of contents for this issue](#), or go to the [journal homepage](#) for more

Download details:

IP Address: 129.252.86.83

The article was downloaded on 27/05/2010 at 20:35

Please note that [terms and conditions apply](#).

Stiffness and thermal expansion of ZrB_2 : an *ab initio* study

V Milman^{1,4}, B Winkler² and M I J Probert³

¹ Accelrys, 334 Science Park, Cambridge CB4 0WN, UK

² Institut für Mineralogie/Abt. Kristallographie, Universität Frankfurt (Main), Senckenberganlage 30, D-60054 Frankfurt, Germany

³ Department of Physics, University of York, Heslington, York YO10 5DD, UK

E-mail: vmilman@accelrys.com

Received 24 November 2004, in final form 24 February 2005

Published 18 March 2005

Online at stacks.iop.org/JPhysCM/17/2233

Abstract

The stiffness and thermal expansion coefficient of ZrB_2 are calculated within the density functional theory formalism. The stiffness tensor obtained here using the static finite strain technique is in good agreement with the results of resonant ultrasonic measurements and points to a possible misinterpretation of the experimentally obtained compression data. The methodology of evaluating thermal expansion coefficients from molecular dynamics simulations for small unit cells is validated for a number of systems: metals, semiconductors and insulators.

1. Introduction

Transition metal diborides with the hexagonal AlB_2 structure have attracted attention recently for a number of reasons. Traditional applications of such materials are based on their interesting combination of mechanical and transport properties: high melting temperature, high stiffness and hardness, high thermal and electrical conductivity [1]. The knowledge of such basic characteristics as stiffness and thermal expansion coefficient is obviously important for applications of ZrB_2 as a refractory material, either on its own or as a matrix of a reinforced composite [2].

Recent advances in GaN optoelectronics have seen ZrB_2 as a promising substrate for epitaxial growth of high quality GaN films [3]. There is very little lattice mismatch between the two materials (0.63%), and their thermal expansion coefficients are also quite similar [1]. The knowledge of elastic and thermal properties of single crystals of ZrB_2 is important for this application. Experimental studies of mechanical and thermodynamical properties of ZrB_2 usually refer to polycrystalline samples, since single crystal growth is difficult in view of the extremely high melting temperature of this compound (3060 °C). To date there exists only

⁴ Author to whom any correspondence should be addressed.

one set of experimental data on single crystal stiffness and thermal expansion coefficients of ZrB_2 [1]. In view of the experimental difficulties in accessing such properties the accuracy of the reported stiffness, for example, can be questionable, as was the case for a similar compound, TiB_2 [4].

The discovery of superconductivity in a related compound, MgB_2 , has prompted a new wave of research into the electronic and structural properties of other diborides, including transition metal diborides. Mahmud *et al* [5] provided a review of the studies relevant to the determination of ZrB_2 properties; they also calculate the stiffness of ZrB_2 using density functional theory (DFT) as implemented in the linear combination of atomic orbitals (LCAO) approach. The results of their LCAO-DFT study are in a generally good agreement with the measured single crystal stiffness coefficients except for the C_{13} component. The deviation of 48 GPa, or 40%, in the C_{13} value is beyond the expected DFT error and indicates that either the calculated or the experimental value is unreliable. The theoretical method chosen by Mahmud *et al* [5] is quite likely to produce inaccurate results for a number of reasons:

- (i) The combination of the local density approximation (LDA) correlation functional with the gradient-corrected exchange functional as adopted by Mahmud *et al* [5] is inconsistent.
- (ii) It is clear that geometry optimization is required for the structures generated with the applied finite strains. Previous studies showed that an error of 2–5% can be assigned to the neglect of this factor [4].
- (iii) The finite strain technique based on the fitting of the total energy as a function of strain is inherently less robust than the one based on the fitting of the stress tensor components (see e.g. [4, 6]). The analysis of the second-order changes in the total energy under applied strain requires very high convergence, which might be difficult to achieve for distortions that lower the symmetry of the crystal.

One of the goals of the present paper is thus to investigate further the discrepancy between the measured [1] and calculated [5] stiffness of ZrB_2 . In addition we would like to analyse the difference of nearly 30% between the reported static [7] and dynamic [1] bulk modulus of ZrB_2 . The static bulk modulus of 317 GPa as determined from the x-ray powder diffraction analysis of compression up to 50 GPa is significantly higher than the value determined from the resonant ultrasonic measurements, 245 GPa [1].

Another physical property of interest which we attempt to calculate from first principles is the coefficient of thermal expansion, α . The approach we adopt here for the determination of α is based on the *ab initio* molecular dynamics calculations using an *NPT* ensemble. Intuitively one expects that a large supercell would be required to extract a reliable temperature dependence of the lattice parameters in such simulations. We show below that for a number of materials (metals, semiconductors, and insulators) the calculations on a conventional unit cell are sufficiently accurate to reproduce the experimental findings qualitatively or even quantitatively (to within 10%).

2. Computational details

ZrB_2 crystallizes in the hexagonal $P6/mmm$ structure with $Z = 1$; the Zr atom is on the 1a Wyckoff site, and the B atoms are on the 2d Wyckoff site [8].

The quantum mechanical calculations described here are based on density functional theory. We use and compare the accuracy of two schemes, the local density approximation, LDA, and the PBE version of the generalized gradient approximation, GGA [9]. Ultrasoft pseudopotentials were used with the maximum cut-off energy of the plane wave basis set of 300 eV. The pseudopotentials were generated using the same exchange–correlation functional

Table 1. Equilibrium structure of ZrB₂. Deviations from the experimental results are given in brackets.

a (Å)	c (Å)	c/a	Comment
3.168	3.523	1.112	Experiment [8]
3.183 (0.5%)	3.546 (0.6%)	1.114	LCAO [5]
3.197 (0.9%)	3.561 (1.1%)	1.114	TB-LMTO [17]
3.167 (−0.1%)	3.542 (0.5%)	1.119	Present work (PBE)
3.127 (−1.3%)	3.490 (−0.9%)	1.116	Present work (LDA)

in the atomic calculations as was used in the solid state calculations. Monkhorst–Pack sampling [10] of the Brillouin zone was used, with distances between the grid points of about 0.03 \AA^{-1} , which corresponds to 95 k -points in the irreducible part of the Brillouin zone.

Stiffness was calculated using the finite strain technique. Two different strain patterns are sufficient to extract all five independent stiffness coefficients of the ZrB₂ structure via linear fitting of the stress–strain dependence [4, 6]. We used four strain amplitudes for each of the patterns, with a maximum applied strain of 0.3%. One of the strain patterns reduces the cell symmetry; in this case atomic positions were optimized until the forces on atoms were below $0.002 \text{ eV \AA}^{-1}$.

NPT molecular dynamics calculations were carried out with a slightly smaller basis set cut-off of 270 eV using two different setups: either the conventional cell with three atoms, or the $2 \times 2 \times 2$ supercell with 24 atoms (*PI* symmetry was used in each case). The equations of motion were integrated using the velocity Verlet scheme [11]. We used the Andersen–Hoover barostat in the form suggested by Hoover [12] coupled with the chain of Nosé–Hoover thermostats approach proposed by Martyna *et al* [14] as implemented by Quigley and Probert [13]. A timestep of 0.5 fs was used and each run was 10 ps long (20 000 steps), with only the last 5 ps being used to determine ensemble averages. All calculations were carried out at atmospheric pressure, $P = 1 \text{ atm}$.

All calculations were performed using the CASTEP program [15, 16].

3. Results and discussion

The structural parameters of ZrB₂ are presented in table 1. The lattice parameters agree with experimental values to within 1%, which is typical for DFT calculations. The results illustrate the well-known qualitative trend of the effect of exchange–correlation treatment on crystal structures: the LDA description produces overbinding (too short interatomic distances), while the GGA description produces underbinding (too long interatomic distances) [18]. The earlier results [5] were obtained with the LDA description of the correlation functional and the gradient-corrected description of the exchange term: this combination seems to generate the typical GGA overbinding effect.

Information about the elastic properties of ZrB₂ can be obtained computationally either from the direct evaluation of the C_{ij} tensor using the finite strain technique, or from a compressibility study. The latter route produces the bulk modulus, B , as well as the linear compressibilities along the a and c directions based on the pressure dependence of the cell volume and lattice parameters, respectively. The linear compressibilities $\beta_a = -d \ln a/dP$ and $\beta_c = -d \ln c/dP$ are related to the elastic stiffness coefficients; see e.g. [4]:

$$\begin{aligned}\beta_a &= (C_{33} - C_{13})/D, \\ \beta_c &= (C_{11} + C_{12} - 2C_{13})/D\end{aligned}\tag{1}$$

where $D = (C_{11} + C_{12})C_{33} - 2(C_{13})^2$.

Table 2. Elastic stiffnesses C_{ij} and bulk modulus B of ZrB_2 . The results obtained here using PBE and LDA approximations are compared to earlier LCAO calculations and to experimental values. The linear compressibilities β_a and β_c are either calculated from the single crystal elastic stiffnesses or they are derived from the compressibility data. The pressure derivative of the bulk modulus, B' , is available only from the compressibility data. C_{ij} and B are in GPa, β_a and β_c are in TPa^{-1} .

C_{11}	C_{33}	C_{12}	C_{13}	C_{44}	B	β_a	β_c	β_a/β_c	B'	Comment
581 ^a	445 ^a	55 ^a	121 ^a	240 ^a	245 ^a	1.28 ^b	1.55 ^b	0.82	—	Experiment [1]
—	—	—	—	—	317(7)	0.87	1.05	0.83	—	Experiment [7] ^c
596	482	48	169	240	272	1.24	1.21	1.02	—	LCAO [5]
—	—	—	—	—	275	1.19	1.25	0.95	3.93	LCAO [5] ^c
—	—	—	—	—	195	—	—	—	1.94	TB-LMTO [17] ^c
564	436	52	118	256	237	1.32	1.58	0.84	—	Present work (PBE)
—	—	—	—	—	238	1.31	1.57	0.83	3.84	Present work (PBE) ^c
606	477	54	134	281	259	1.23	1.41	0.87	—	Present work (LDA)
—	—	—	—	—	260	1.22	1.41	0.87	3.85	Present work (LDA) ^c

^a Extrapolated to 0 K by us based on the results from [1].

^b Calculated using equation (1).

^c Based on the compressibility data.

A summary of the present results is presented in table 2 in comparison with the experimental data and with the earlier results of the LCAO study [5]. The third-order Birch–Murnaghan equation of state [19] was used to analyse the calculated compression data. The pressure dependence of the lattice parameters and thus of the cell volume was constructed by carrying out geometry optimization under applied external pressure.

The main question addressed by the bulk modulus calculation is which experimental value is more reliable: the equation of state result of 317(7) GPa [7], or the value of 245 GPa derived from the ultrasonic measurements [1]. This discrepancy between the two sets of data is unusually large to be ascribed to the difference between the static and dynamic moduli. The results obtained here support the value of 245 GPa. The PBE calculation which slightly overestimates the cell volume produces $B = 237$ GPa, while the LDA calculation that uses slightly underestimated cell parameters gives a higher value of $B = 259$ GPa. This relationship is consistent with the previous studies of the effect of the exchange–correlation functional on the calculated equation of state [4, 6, 18]. The overbinding of the LDA approach results in overestimated bulk moduli, while gradient-corrected functionals like PBE underbind and consequently produce too low bulk moduli. The fact that our two results obtained with LDA and GGA exchange–correlation functionals are so close to the experimental result of Okamoto *et al* [1] strongly suggests that the full stiffness tensor measured by those authors represents a reliable set of material parameters of ZrB_2 . Note that internal consistency of the present results is illustrated by the comparison of the bulk modulus values and the linear compressibilities calculated from the C_{ij} tensor and from the compression data, table 2. The discrepancy between the two sets of results is less than 0.5%.

The results of the LCAO study [5] fall essentially between the two sets of the experimental values for the bulk modulus. The LCAO results fail to reproduce the experimentally observed anisotropy of the compression of ZrB_2 . Both experiments, as well as our PBE calculation, show that the c axis is about 20% more compressible than the a axis, while the results of Mahmud *et al* [5] give essentially isotropic compressibility (table 2).

The only other DFT calculation of the compressibility of ZrB_2 that we are aware of has been carried out using the tight binding LMTO method with the LDA description of the exchange–correlation [17]. This calculation produced a very low bulk modulus of 195 GPa,

while the cell parameters were overestimated by more than 1%. An underbinding in an LDA calculation points towards some fundamental technical problems of the method employed by Vajeeston *et al* [17]. We have shown above, see tables 1 and 2, that properly converged calculations confirm the general trend of LDA overbinding and GGA underbinding in the solid state. In addition, the value of the pressure derivative of the bulk modulus, B' , is very low according to [17]. This value is close to 4 for most inorganic materials; in fact, it is often set to 4 for the purposes of fitting an analytical equation of state to low quality experimental data, as was the case in the study of Pereira *et al* [7]. Both present and earlier results agree with this estimate (table 2), while the TB-LMTO study [17] obtained B' between 1 and 2 for 12 transition metal diborides. In our opinion, the underbinding within the LDA approach together with the unrealistically low values of B' make the results for ZrB₂ obtained by Vajeeston *et al* [17] unreliable.

The coefficients of thermal expansion (CTEs) of ZrB₂ have been determined in the temperature range from room temperature to 1073 K by Okamoto *et al* [1]. The CTE values averaged over the temperature range indicate a nearly isotropic expansion of the hexagonal ZrB₂ structure: $\alpha_a = 6.66 \times 10^{-6} \text{ K}^{-1}$ and $\alpha_c = 6.93 \times 10^{-6} \text{ K}^{-1}$. The actual dilatometry data analysed by Okamoto *et al* [1] are quite noisy, and the error bars on the reported average values are of the order of $0.3 \times 10^{-6} \text{ K}^{-1}$. In fact, if we consider the temperature dependence of the reported CTEs, then we find that $\alpha_a > \alpha_c$ starting from 673 K. This experimentally observed isotropic behaviour is unusual for a hexagonal crystal, and it justifies the use of the Andersen–Hoover barostat to carry out molecular dynamics in the *NPT* ensemble with the fixed cell shape.

The CTEs are rarely determined from *ab initio* molecular dynamics calculations, thus we tested the technique before applying it to ZrB₂. The isotropic expansion of a number of simple substances with cubic symmetry was studied using the conventional cell description (4 or 8 atoms per FCC cell, 2 atoms per BCC cell). The energy cut-off and Brillouin zone sampling were chosen to produce lattice parameters that converged to better than 0.0001 Å. A series of MD runs has been performed for each material at 5–7 temperatures spanning the temperature range of interest. Each run contained 10 000 steps with a time step of 0.1–0.5 fs. The comparison of the results obtained with different time steps showed that 0.5 fs is sufficient for conserving the constant of motion, so this value was used in the subsequent studies of ZrB₂. The cell parameter for a given temperature was determined by simple averaging over the second half of the MD run. The linear fit of the resultant $a(T)$ dependence produced the CTE value as well as the value of the lattice parameter extrapolated to $T = 0 \text{ K}$.

The results given in table 3 show that even extremely small cells used in these tests are capable of producing qualitative and even quantitative agreement with experiment. There is a substantial scatter of the calculated data, resulting in the statistical uncertainty of the theoretical CTE of the order of 10%. One expects that the increase of the simulation cell should reduce this scatter.

One further comment should be made with regard to the comparison of calculated and measured CTE values (table 3). The CTEs for the investigated compounds are usually temperature dependent. The variation of CTEs in the range of temperatures we used, 200–800 K, can be quite large: from 1.5 to $4.0 \times 10^{-6} \text{ K}^{-1}$ for diamond [21, 22]; 23 to $33 \times 10^{-6} \text{ K}^{-1}$ for Al [23]; 4 to $4.8 \times 10^{-6} \text{ K}^{-1}$ for W [24], etc. The quality of the data obtained in the MD calculations is insufficient to attempt a more sophisticated analysis than the linear fit over the entire temperature range, and thus the only meaningful comparison is against the average experimental CTE values.

The values of lattice parameter extrapolated to $T = 0 \text{ K}$ agree well with the results of the static geometry optimization (table 3). The discrepancies between the extrapolated and static

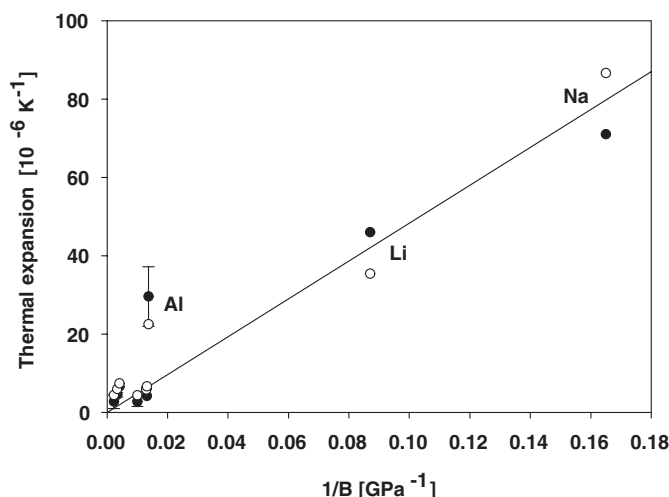


Figure 1. Correlation between the linear coefficients of thermal expansion and compressibility for the materials studied in table 3 (○—theory, ●—experiment [20]). The bulk modulus values are taken from [25], except for Ge [26] and AlAs [27]. For Al, the experimentally observed temperature dependence of the CTE is significant and is indicated by a vertical bar. The temperature dependence of the CTE of diamond and tungsten is comparatively small and corresponds approximately to the symbol size.

Table 3. Calculated linear coefficients of thermal expansion for cubic crystals (in 10^{-6} K^{-1}). Experimental data [20] refer to 300 K. The lattice constants obtained from the extrapolation to $T = 0 \text{ K}$, a_{ext} , are compared to the results of a direct geometry optimization, a_{opt} .

Material	Theory	Experiment	a_{ext} (Å)	a_{opt} (Å)
Si	4.4	4.7	5.396	5.385
Ge	5.8	6.1	5.550	5.553
C (diamond)	4.4	1.2	3.536	3.536
AlAs	6.6	4.2	5.600	5.592
Al	22.5	23.1	3.969	3.957
Li	35.4	46.0	3.428	3.430
Na	86.6	71.0	4.280	4.289
W	6.0	4.5	3.224	3.222

values are due most likely to the limitation of the extrapolation procedure, which assumes temperature-independent CTEs.

It is instructive to verify how well the calculated and experimental CTE values from table 3 follow the theoretical dependence on other thermodynamical material properties [20]:

$$\alpha = \gamma C_V / BV, \quad (2)$$

where $\gamma = C_P / C_V$ is the heat capacity ratio, C_V is the heat capacity at constant volume, B is the bulk modulus, V is the volume. The value of γ is typically close to 1 for solids, and C_V can be treated as a constant at elevated temperatures. The unit cell volumes of the materials listed in table 3 are similar, so one expects an inverse proportionality between the thermal expansion coefficient and the bulk modulus. This qualitative dependence predicted by equation (2) can indeed be seen in figure 1: the more compressible materials such as Li and Na possess the highest CTE. The deviation between the calculated and experimental CTE values is also the

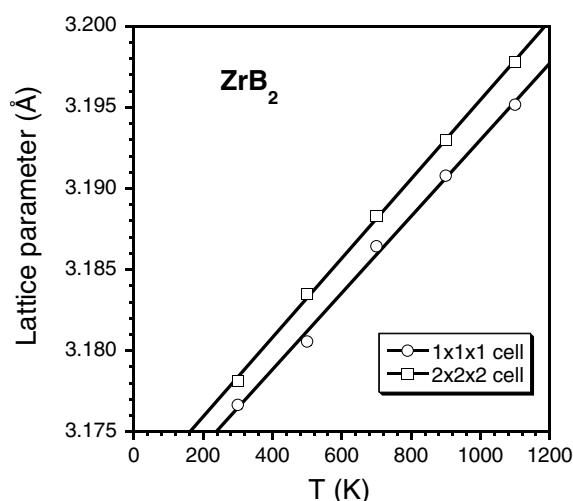


Figure 2. Temperature dependence of the a lattice parameter of ZrB₂ calculated using the 3-atom cell (○) and the 24-atom cell (□).

highest for the crystals with low bulk modulus. This is partially due to bigger fluctuations that lead to higher error bars for the calculated CTEs in soft materials.

The values of the lattice parameters extrapolated to $T = 0$ K agree very well with the values obtained from geometry optimization. The largest discrepancy is observed for Li, where one expects vibrational effects to be more important in view of its small atomic mass. The results overall are encouraging for applications of the Andersen–Hoover barostat to CTE calculations for isotropic crystals.

A protocol similar to the one described above has been applied for hexagonal ZrB₂. The time step was chosen as 0.5 fs, each run was 10 ps long (20 000 steps) and the last 5 ps were used to determine the average lattice parameter. We used five different temperatures from 300 to 1100 K for linear fitting of the $a(T)$ dependence; see figure 2. We obtained the CTE of $7.4(5) \times 10^{-6} \text{ K}^{-1}$, in satisfactory agreement with the experimental result [1]. The extrapolation to $T = 0$ K produces $a = 3.169 \text{ Å}$, in good agreement with the result of direct geometry optimization (see table 1).

We have verified that the agreement with experiment is not fortuitous by repeating the calculation for the $2 \times 2 \times 2$ supercell containing 24 atoms. These calculations are clearly more demanding computationally, since the scaling of the plane wave pseudopotential technique with the number of atoms is of the order of N^2 to N^3 . This scaling implies that the cost of a calculation on such a supercell should be 100–500 times higher than on the original cell. In fact, the effect of increasing the cell is made less costly by the reduction of the number of k -points required for the Brillouin zone sampling. This number is reduced by a factor of ~ 6 , and the overall observed increase in the computational time is of the order of only 50, making the calculations feasible. We have halved the number of steps in the supercell calculations so that the length of the runs was now 5 ps.

The thermal expansion calculated for the $2 \times 2 \times 2$ supercell (figure 2) is described with the CTE of $7.7(3) \times 10^{-6} \text{ K}^{-1}$, thus confirming that the 3-atom cell generates sufficiently accurate thermal expansion data. The lattice constant extrapolated to 0 K is slightly different in these calculations ($a = 3.171 \text{ Å}$) compared to the small cell results; however, the discrepancy is well within the expected accuracy limits. The statistical error in the calculated CTE is slightly

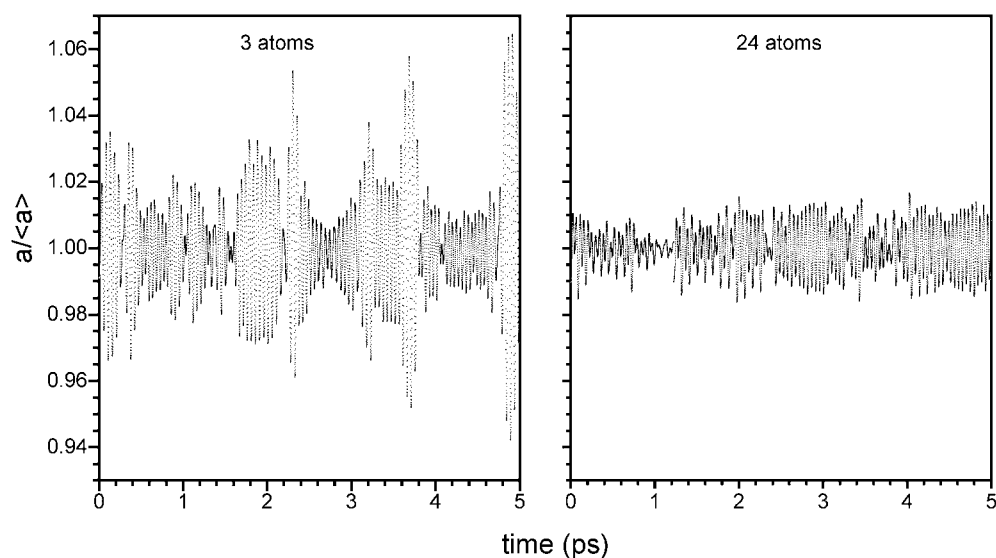


Figure 3. Comparison of the time evolution of the ZrB_2 cell parameter, a , in the MD calculations at $T = 1100$ K using the 3-atom cell (left panel) and the 24-atom cell (right panel). The cell parameter is given relative to the average value of the production run. Only the last 5 ps of each simulation are shown.

lower in the supercell calculation as one expects intuitively. This effect is due partly to a better quality of the linear fit (see figure 2), and partly to the reduced standard deviation of the time-averaged cell parameter in each individual MD run. The latter effect is demonstrated by figure 3, which shows that the standard deviation is reduced by a factor of 2–3 when we use the 24-atom supercell.

4. Conclusions

We have reported density functional results for the elastic properties and thermal expansion coefficients of a promising technological material ZrB_2 . The calculated stiffness is in good agreement with the experimental values obtained using the resonance ultrasonic technique [1]. These results indicate that the conclusions of the high-pressure study by Pereira *et al* [7] are unreliable and need further examination.

We showed that the *NPT* dynamics calculation, even for extremely small cells, is capable of describing thermal expansion coefficients.

Acknowledgment

BW would like to thank the Deutsche Forschungsgemeinschaft for funding through grant Wi1232/12.

References

- [1] Okamoto N L, Kusakari M, Tanaka K, Inui H, Yamaguchi M and Otani S 2003 *J. Appl. Phys.* **93** 88
- [2] Brown A S 1997 *Aerosp. Am.* **35** 20
- [3] Iwata J I, Siraishi K and Oshiyama A 2003 *Phys. Status Solidi c* **0** 2482

-
- [4] Milman V and Warren M C 2001 *J. Phys.: Condens. Matter* **13** 5585
- [5] Mahmud S T, Islam A K M A and Islam F N 2004 *J. Phys.: Condens. Matter* **16** 2335
- [6] Milman V and Warren M C 2001 *J. Phys.: Condens. Matter* **13** 241
- [7] Pereira A S, Perottoni C A, Jornada J A H da, Leger J M and Haines J 2002 *J. Phys.: Condens. Matter* **14** 10615
- [8] Epelbaum V A and Gurevich M A 1958 *Zh. Fiz. Khim.* **32** 2274
- [9] Perdew J P, Burke K and Ernzerhof M 1996 *Phys. Rev. Lett.* **77** 3865
- [10] Monkhorst H J and Pack J D 1976 *Phys. Rev. B* **13** 5188
- [11] Swope W C, Andersen H C, Berens P H and Wilson K R 1982 *J. Chem. Phys.* **76** 637
- [12] Hoover W G 1985 *Phys. Rev. A* **31** 1695
- [13] Quigley D and Probert M I J 2004 *J. Chem. Phys.* **120** 11432
- [14] Martyna G J, Tuckerman M E, Tobias D J and Klein M L 1996 *Mol. Phys.* **87** 1117
- [15] Accelrys Inc. 2003 *CASTEP User Guide* (San Diego, CA: Accelrys Inc.)
- [16] Segall M D, Lindan P J D, Probert M I J, Pickard C J, Hasnip P J, Clark S J and Payne M C 2002 *J. Phys.: Condens. Matter* **14** 2717
- [17] Vajeeston P, Ravindran P, Ravi C and Asokamani R 2001 *Phys. Rev. B* **63** 045115
- [18] Broqvist P, Grönbeck H and Panas I 2004 *Surf. Sci.* **554** 262
- [19] Birch F 1947 *Phys. Rev.* **71** 709
- [20] Lide D R *et al* (ed) 1993 *Handbook of Chemistry and Physics* 73rd edn (Boca Raton, FL: CRC Press)
- [21] Slack G A and Bartram J 1975 *J. Appl. Phys.* **46** 89
- [22] Reeber R R and Wang K 1996 *J. Electron. Mater.* **25** 63
- [23] Wilson A J C 1941 *Proc. Phys. Soc.* **53** 235
- [24] Plöchl L 1995 Plansee Aktiengesellschaft, Reutte, Austria (unpublished)
<http://www-ferp.ucsd.edu/LIB/PROPS/ITER/AM01/AM01-3114.html>
- [25] Ahrens T J 1995 *A Handbook of Physical Constants: Mineral Physics and Crystallography* vol 2 (AGU Reference Shelf)
- [26] Srivastava G P and Weaire D 1987 *Adv. Phys.* **36** 463
- [27] Greene R G, Luo H, Li T and Ruoff A L 1994 *Phys. Rev. Lett.* **72** 2045